Synthesis of Crosslinkable Latices with Poly(vinyl acetate-*co*-VeoVa10) Cores and Poly(glycidyl methacrylate) Shells and Online-FTIR Analysis of the Amine Induced Curing Process

Jia Lu, Allan J. Easteal, Neil Edmond

Department of Chemistry, Centre for Advanced Composite Materials, University of Auckland, Auckland, New Zealand

Received 27 February 2011; accepted 4 May 2011
DOI 10.1002/app.34837
Published online in Wiley Online Library (wileyonlinelibrary.com).

ABSTRACT: Crosslinkable latex particles with poly(vinyl acetate-*co*-VeoVa10) core and poly(glycidyl methacrylate) shell were synthesized by emulsion polymerization. Starved feed and seed emulsion polymerization were used to control the morphology of the core-shell latex particles. The effect of emulsifier concentration, chain transfer agent, and starved feeding on the core-shell morphology were investigated. The formation of core-shell particles was promoted by increasing seed particle numbers and by the starved-feed condition. Investigation of isothermal crosslinking of the core-shell latex and the curing agent Anquamine 419 (a modified aliphatic amine), using real-time Fourier transform infrared spectroscopy, revealed that the cure rate was relatively low at ambient temperature, but curing was complete within about 4 h at 30°C and about 1.5 h at 40°C. © 2012 Wiley Periodicals, Inc. J Appl Polym Sci 000: 000–000, 2012

Key words: emulsion polymerization; core-shell polymers; crosslinking; vinyl acetate; glycidyl methacrylate

INTRODUCTION

The synthesis of core-shell particles in emulsion polymerization has attracted scientific and industrial interest because structured composite latex particles have different, and in many cases more desirable properties than the corresponding blends or copolymers. In this study, the synthesis of a core-shell latex comprising cores of a copolymer of vinyl acetate (VAc) and VeoVa10, and poly(glycidyl methacrylate) (PGMA) shells was investigated.

This system was chosen for study because poly(vinyl acetate) (PVAc)-based latexes are the most widely used wood adhesives. However, PVAc has the disadvantages of poor water-, creep-, and heat resistance. There are several approaches to circumventing these problems. One approach is copolymerization of VAc with hydrophobic monomers such as methyl methacrylate (MMA)[1] and butyl acrylate,[2] to reduce the moisture sensitivity of the backbone chains. Another effective and widely used strategy is incorporation of isocyanates such as polyisocyanate[3] in the PVAc emulsion immediately before use. The isocyanate functional groups react relatively rapidly with OH groups on the (partially hydrolyzed) PVAc chains, thereby creating crosslinks between chains. The major disadvantage of isocyanate-modified PVAc adhesives is the hazards associated with use of isocyanates. Blending PVAc emulsions with thermosetting resins melamine-formaldehyde[4] and melamine-urea-formaldehyde[4] is also effective but hazardous due to formaldehyde emission.

Glycidyl methacrylate (GMA) is a very useful reactive monomer because it contains both a pendant epoxide group and an unsaturated group and can be used in either nucleophilic substitution reactions or in radical initiated reactions, and the epoxy group provides postcrosslinking potential. However, because of the unfavorable comonomer reactivity ratios of VAc ($r_v = 0.03$) and GMA ($r_G = 39.5$),[5] copolymers of VAc and GMA cannot easily be made with comparable proportions of VAc and GMA units. Consequently, the strategy of creating core-shell particles to introduce GMA units into the seed PVAc latex is attractive, because it might be possible to retain the film-formation properties of PVAc latex, leaving PGMA shells to provide crosslinking sites with curing agents which might give improved water-, heat-, and creep resistance. There are many reports on noncrosslinkable core-shell structured latexes, including polystyrene/PVAc,[6–8] polystyrene/poly(butyl acrylate),[9] polystyrene/PMMA,[10] polystyrene/poly(pyridyl methacrylate),[11] poly(butyl

Correspondence to: J. Lu (jlu046@aucklanduni.ac.nz).

methacrylate)/poly(methacrylic acid),[12] and poly (methyl methacrylate-ethyl acrylate)/poly(methacrylic acid) latexes,[13] but no reports, so far as we are aware, on crosslinkable PVAc-based core-shell latexes.

EXPERIMENTAL SECTION

Chemicals

Vinyl acetate and VeoVa10 were supplied by Nuplex Chemicals, Auckland New Zealand. Inhibitor was removed from VAc by passing the monomer through a column packed with quaternary ammonium anionic exchange resin (Aldrich Chemical), the first and last 10% fractions being discarded. GMA and VeoVa10 were purified by distillation under reduced pressure, the first and last 10% of the distillate being discarded. All monomers were stored in darkness at 2°C for not longer than a week before use. Anquamine 419 was supplied as a 60% solids dispersion in water/methoxy propanol by TCL Hunt, Auckland, New Zealand. All other reagents were used as received. The radical initiators ammonium peroxydisulfate (APS) (Aldrich Chemicals) and benzoyl peroxide (BPO) (BDH Chemicals), chain transfer agent (CTA) 1-dodecanethiol (DDM) (Aldrich Chemicals), sodium dodecylbenzene sulphate (SDBS) emulsifier and sodium hydrogen carbonate buffer were used as received.

Polymerization

The seed latex, poly(VAc-*co*-VeoVa10) emulsion, was prepared via semicontinuous emulsion polymerization at 75°C for 4 h using 200 g deionized water, 80 g VAc, 16 g VeoVa10, 0.48 g APS and 0.1 g $NaHCO_3$, with varying amounts of SDBS and DDM.

Core-shell latexes were prepared with PVAc/VeoVa10 as the seed; 19 g GMA monomer was added in a starved feed process with BPO as initiator. The formulation is shown in Table I.

The syntheses were performed in a 500 mL five-neck glass reactor. SDBS and $NaHCO_3$ were weighed into a beaker with deionized water and stirred until the emulsifier and $NaHCO_3$ had dissolved. Half of the mixture was then added to the reactor. The VAc, VeoVa10, and DDM were weighed into a beaker with the remaining half of the mixture, and the pre-emulsion of monomers was stirred for 10 min. The reactor was heated to the reaction temperature, stirring was begun, and a flow of high purity nitrogen was started to flush oxygen from the reactor. When the reactor had attained the set temperature, the initial charge of APS, dissolved in a small quantity of deionized water, was added followed immediately by the initial charge of the monomer pre-emulsion. The reactor was sealed and stirred for 40 min. A gradual feed of the remaining pre-emulsion was begun at 70 mL h^{-1}, during which APS solution was added to the reactor at 30-min intervals. When the addition of APS was complete, reaction was continued for 1 h to allow polymerization of remaining monomer. The temperature was then reduced to ambient temperature, and the reaction mixture stirred for at least 8 h. The reactor was then heated to 50°C, and 19 g GMA was added dropwise. BPO (0.2 g) was dissolved in GMA and added to the reactor with GMA. The reaction was allowed to proceed for a further 60 min after completion of the monomer feed.

TABLE I
Formulation for Emulsion Polymerization

	Component	Weight (g)
First stage polymerization	DS10	0.52–8.9
	Water	180
	Vinyl acetate	85
	VeoVa 10	15
	1-dodecanethiol (DDM)	0.1–1.0
	Ammonium persulfate (APS)	0.75
	Water	5
	Tert-butylhydroperoxide (TBHP)	0.004
	Water	1
	Sodium formaldehyde sulphoxylate (SFS)	0.004
	Water	1
Second-stage polymerization	Benzoyl peroxide (BPO)	0.07–0.80
	Glycidyl methacrylate	7–80

Characterization

The morphology of latex particles was examined using a transmission electron microscope (TEM) (Philips model CM12 from FEI Company, Eindhoven, The Netherlands) equipped with a Bioscan digital camera (Gatan, Inc., Pleasanton, CA). Uranyl acetate was used as a negative staining agent. Latex particle size and particle size distributions were determined using a Mastersizer 2000 instrument (Malvern Instruments). The compositions of seed copolymer and core-shell polymer particles were determined by NMR spectroscopy using a Bruker Avance 400 instrument.

Real-time Fourier transform infrared measurements of isothermal postcrosslinking process

The core-shell emulsion and commercial curing agent Anquamine 419 (with amine value 284 mg KOH g^{-1}) were mixed in the stoichiometric ratio of amino groups to epoxy groups. Fourier transform infrared (FTIR) spectra were obtained with a Thermo Electron Nicolet 8700 FTIR spectrometer equipped with ZnSe crystal beamsplitter and a variable temperature stage. The spectra were collected every 52 s during crosslinking, over a period of 3 h, at 22, 30, and 40°C.

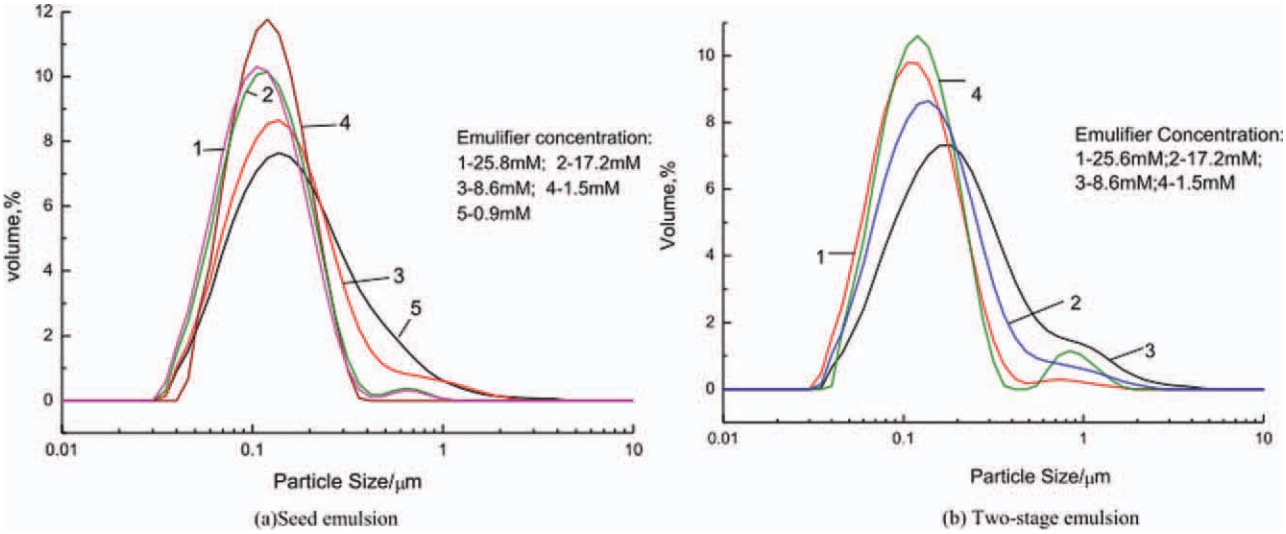

Figure 1 Variation of particle size distribution with emulsifier concentration, for (a) seed emulsion and (b) core-shell emulsion. [Color figure can be viewed in the online issue, which is available at wileyonlinelibrary.com.]

RESULTS AND DISCUSSION

Effect of emulsifier concentration on particle size and particle morphology

The formation of core-shell morphology was influenced primarily by the seed concentration and particle size, because the overall rate of entry for active radical species is proportional to particle size and number of particles during the two stage emulsion polymerization (of GMA).[8] Hence, it is essential to control the emulsifier level in the preparation of seed latex to attain the optimum number and size of seed particles. To achieve a core-shell structured latex and avoid secondary nucleation, the second-stage emulsion polymerization was implemented without further addition of emulsifier. The SDBS concentrations used in the seed latex were 25.8, 17.2, 8.6, 1.5, and 0.9 m*M*, the latter being below the critical micelle concentration (CMC; 1.5 m*M*), while the concentrations of the other components were kept constant.

Figure 1(a) shows that the particle size of the seed emulsion was dictated by the emulsifier concentration at constant solids content, under steady-state emulsion polymerization conditions. Above the CMC, the particle sizes and their distributions (curves 2–5) shifted slightly toward decreased average particle size as the emulsifier concentration increased. Above the CMC, micellar nucleation was favored over homogeneous nucleation by at least 10 orders of magnitude.[14] According to the micellar nucleation model, particle numbers are proportional to the initial emulsifier concentration.[14] Below the CMC, the combination of instability and coagulation resulted in a broader distribution and larger particle size.

Figure 1(b) shows (in curves 1, 2, and 3) that the core-shell emulsions made from the seed emulsion with emulsifier concentration above the CMC had unimodal particle size distribution. Below the CMC, the second stage starved polymerization was incomplete due to aggregation and coagulation. At the CMC [curve 4 in Fig. 1(b)], a bimodal distribution of particle sizes appeared for the core-shell emulsion. Figure 2 reveals that above the CMC the average particle size of the core-shell emulsion was clearly larger than that of the corresponding seed emulsion: in both cases, the particles had unimodal size distribution. These results imply that in the second stage monomer polymerized mostly on the surface of the seeds and generated core-shell structured particles. TEM images (Fig. 3) confirmed the predominantly core-shell morphology. Comparison of the particle morphology of the seed emulsions with emulsifier concentrations 17.2 m*M* [Fig. 3(a)] and 8.6 m*M* [Fig. 3(c)] and the corresponding core-shell emulsions [Fig. 3(b,d)] shows that the two-stage emulsions had core-shell structures, and the seed latex particles were smaller than the core-shell particles. In the TEM images, the brighter poly(VAc-*co*-VeoVa10) domains can be clearly differentiated from the dark PGMA areas. In the seeded starved emulsion polymerization, the viscosity in the seed was very high, so radicals had difficulty entering the latex particles and polymerization occurred place at the seed-water interface. The morphology in Figure 3(e,f) indicates that core-shell structures were not generated with seed latex with 1.5 m*M* emulsifier concentration, confirming that creation of core-shell particles was controlled by the number and size of seed particles. The seed emulsion with 1.5 m*M* emulsifier concentration had a larger average particle size than those with the 8.7 and 17.2 m*M* emulsifier concentrations (Fig. 2). With constant solids constant, as seed size

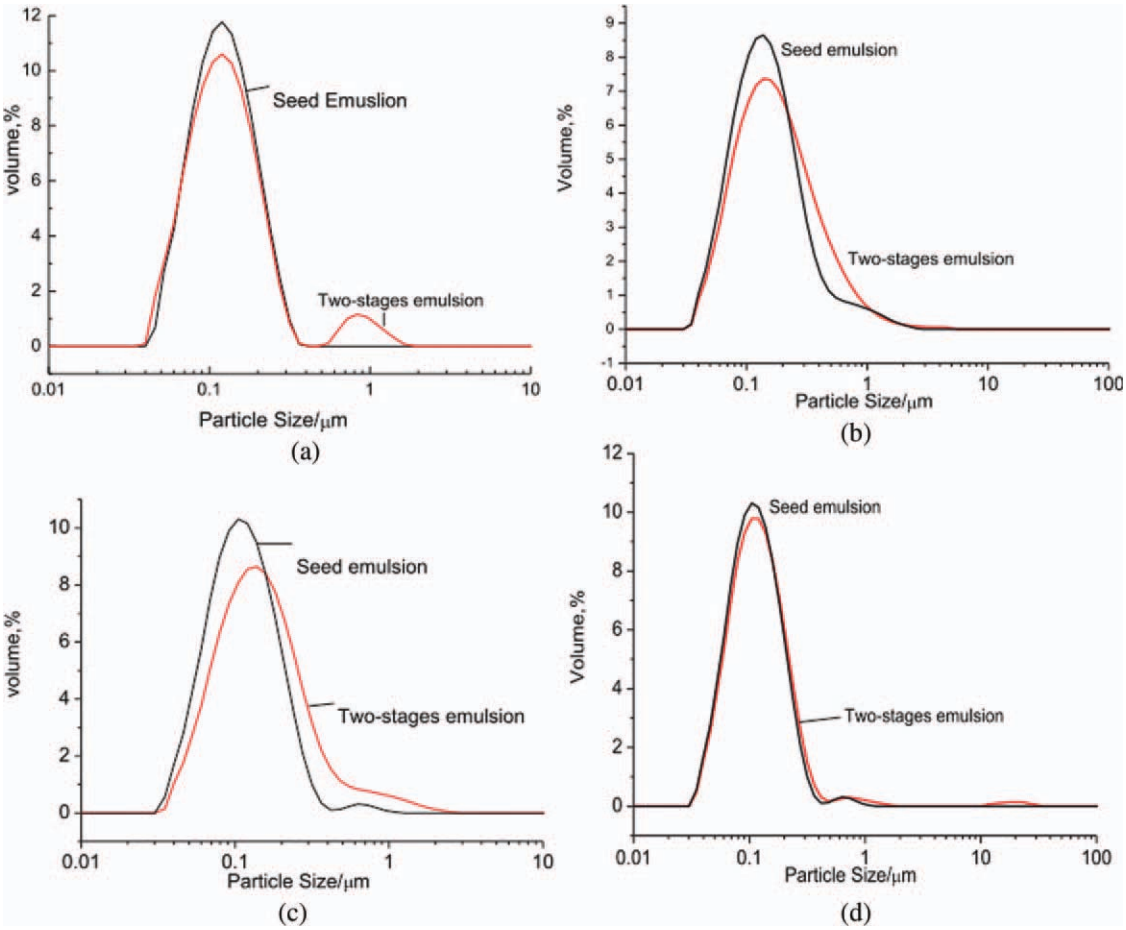

Figure 2 Comparison of particle size distributions of seed emulsion and core-shell emulsions. Emulsifier (SDBS) concentration in seed emulsion: (a) 8.6, (b) 17.2, (c) 25.6, and (d) 1.5 m*M*. [Color figure can be viewed in the online issue, which is available at wileyonlinelibrary.com.]

was reduced, the increase in the number of particles (which is inversely proportional to the cube of particle radius) far outweighed the decrease in particle size, so the number of particles of the seed emulsion with 1.5 m*M* emulsifier concentration was much less than in the seed emulsions with 8.7 and 17.2 m*M* emulsifier concentrations. The overall opportunities for radicals entering pre-existing particles were reduced, and secondary nucleation increased as the seed emulsifier concentration was reduced. On the basis of the particle morphologies shown in Figure 3, it seems that an intermediate concentration of emulsifier (of the order 10 m*M*) gives the best balance between core-shell formation and formation of acorn particles.

NMR analysis of core-shell particles

Figure 4 shows the ^{1}H-NMR spectrum of a composite of poly(VAc-*co*-VeoVa10) and poly(GMA) with 11 mol % GMA units. The methine protons of the VAc and VeoVa 10 units appear at 4.89 ppm. The oxymethylene protons of GMA units gave broad signals at 3.96 and 4.29 ppm, and the epoxy methylene proton signals of GMA units appeared at 2.65 and 2.79 ppm. The epoxy methine protons of GMA units gave a signal at 3.20 ppm. The ester methyl group proton signals of the VAc units appeared in the 2.1–1.7 ppm range as a signal overlapped with signals from the backbone methylene protons of VeoVa10 units, both appearing as multiplets at 1.6–1.0 ppm. The resonance signal of methyl protons of Veo Va 10 and methyl protons connected with the backbone of GMA units appeared at about 0.9 ppm. The peak at about 4.89 ppm is from methine proton resonances of VAc and Veo Va10 units. The doublet peaks at 2.65 ppm and 2.79 ppm are from the methylene protons resonances of GMA units. The molar proportion of GMA in the core-shell particle was calculated from the relative intensities (relative areas) of the methine signal of copoly(VAc-VeoVA10) and the epoxy methylene resonance of PGMA via eq. (1)

$$\text{mol \% GMA} = \{(I_{2.6} + I_{2.8})/2\}/[\{(I_{2.6} + I_{2.8})/2\} + (I_{4.89}/1.08)] \quad (1)$$

where $I_{2.6}$ and $I_{2.8}$ are the intensities of the epoxy methylene proton signals of the GMA unit, and $I_{4.89}$

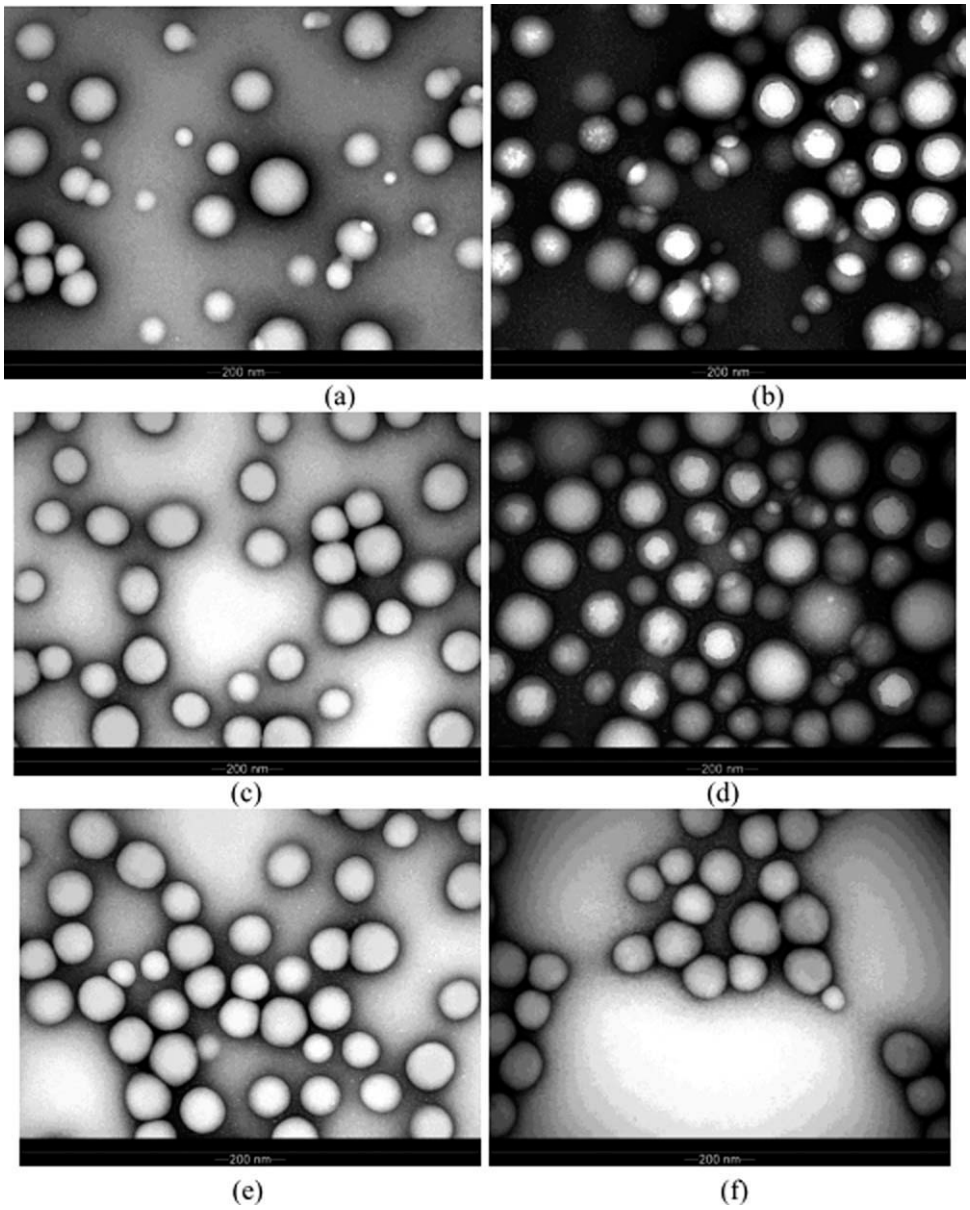

Figure 3 TEM images of seed and core-shell emulsions. Seed emulsions with SDBS concentration: (a) 17.2, (c) 8.6, and (e) 1.5 mm. Images (b), (d), and (f) refer to core-shell emulsions made from seed emulsions (a), (c), and (e), respectively.

is the intensity of the methine proton (backbone) signal of the copolymer of VAc and Veo Va10. In terms of the composition of copoly(VAc/Veo Va10), it was estimated that 1 mol of copolymer contained on average 1.08 mol methine protons.

Effect of CTA on particle size and particle morphology

There is good reason to suspect that seed polymer immobility is an important factor in determining the morphology. With the aim of varying seed polymer immobility, a series of experiments were performed in which the CTA DDM was used in copolymerization of VAc and VeoVa10 to form the seed latex. Five DDM/monomer ratios were used while the concentrations of other components were kept constant. The molar mass data in Table II show that the addition of DDM had a strong influence on the number average molecular weight (M_n) of the seed polymer, particularly at higher DDM concentration. As DDM has very low solubility in water, it is assumed that the DDM is located wholly in the seed latex particles. In that case the average length of the seed polymer chains, and hence the average molar mass, was expected to be reduced to an increasing extent with increasing DMM concentration, as observed. Figure 5(a) shows the strong influence of DDM concentration on seed particle size distribution; the distribution narrowed dramatically with

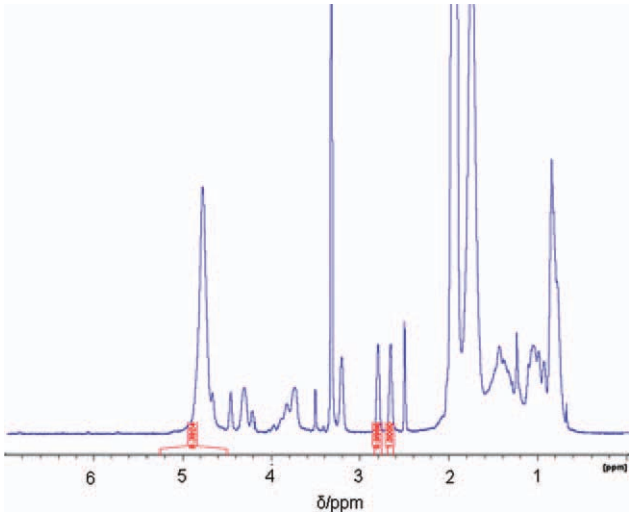

Figure 4 1H-NMR Spectrum of composite of copolymer of VAc/VeoVa 10 and PGMA with 11 mol % GMA units. [Color figure can be viewed in the online issue, which is available at wileyonlinelibrary.com.]

increasing DDM concentration. By contrast, variation of the DDM concentration had much less effect [Fig. 5(b)] on the core-shell particle size distribution.

The diameters of both seed and core-shell particles decreased substantially with addition of up to 0.3 wt % DDM but changed little with further addition of DDM (Table II). Thus, assuming an idealized (concentric spherical) core-shell structure the thickness of the shell was essentially constant at 27 ± 3 nm for DDM concentrations from 0.3 to 1 wt %.

One contribution to the decrease in the number average molecular weight (M_n) of the seed polymer with increasing DDM concentration might be increased rate of escape of chain-transferred radicals from the polymer particles. It has been proposed that in the emulsion polymerization of vinyl pivalate, there is a decrease in the average number of radicals per particle, in the presence of a CTA with very low solubility in water, and enhanced desorption of CTA radicals from the polymer particles.[15] The considerable increase of radical desorption from the particles produced by CTA affords a decrease of the degree of polymerization of the resulting polymer.[15,16]

Figure 6 shows that some acorn (multicore) structures appeared in the core-shell emulsion, and there was a greater proportion of particles with acorn morphology in the presence of the CTA than in its absence [compare Fig. 6(b,c,d) with Fig. 6(a)]. In addition, it seemed that the proportion of particles with acorn morphology increased with increasing concentration of CTA, particularly for the highest concentration of CTA. Due to reduction of the length of the seed polymer chains in the presence of CTA, the polymer chains should be more mobile and the viscosity of the latex reduced, in the presence of CTA. Enhanced diffusion within the particles may mean that the morphology was controlled more by thermodynamic considerations than by kinetic restrictions.[16,17] Thus, by using DDM in the seed synthesis the key change was the chain architecture; shorter seed polymer chains, diffusing more rapidly than in the absence of CTA. In addition, residual unreacted DDM would reduce the average PGMA chain length in the second stage polymerization. Reduction of the average length of the seed polymer chains or polyGMA chains increases the probability of both diffusing into or out of seed latex particles. Consequently, the probability of secondary nucleation and occurrence of multicore morphology is greater in the presence of CTA.

Use of DDM in the first stage of the emulsion polymerization thus provided control of seed polymer molecular weight, and seed particle size and size distribution. However, DDM had a deleterious effect on the morphology of the core-shell polymer particles,

Effect of starved feed of GMA monomer

To avoid secondary nucleation in the second stage emulsion polymerization, the overall rate of polyGMA chain propagation can be reduced by decreasing the GMA concentration. A large reduction in GMA concentration was achieved by operating under so-called starved feed conditions. This term generally means that the monomer is being added more slowly than its rate of consumption if the system were saturated with monomer. This requires

TABLE II
Effect of Chain Transfer Agent (DDM) Concentration on M_n (seed) and Average Seed and Core-Shell Particle Diameters

DDM/monomer (wt %)	M_n (kg mol^{-1}) (seed)	d (nm) (seed)	d (nm) (core-shell)	Shell thickness (nm)
0	–	198	356	79
0.1	369.1	169	257	44
0.3	291.8	151	199	24
0.6	223.2	137	190	27
1	42.2	142	202	30

M_n is the number average molar mass of the seed polymer; and d is average particle diameter of the latex. M_n data for the sample without chain transfer agent were not obtained due to the very small solubility of that sample in DMSO.

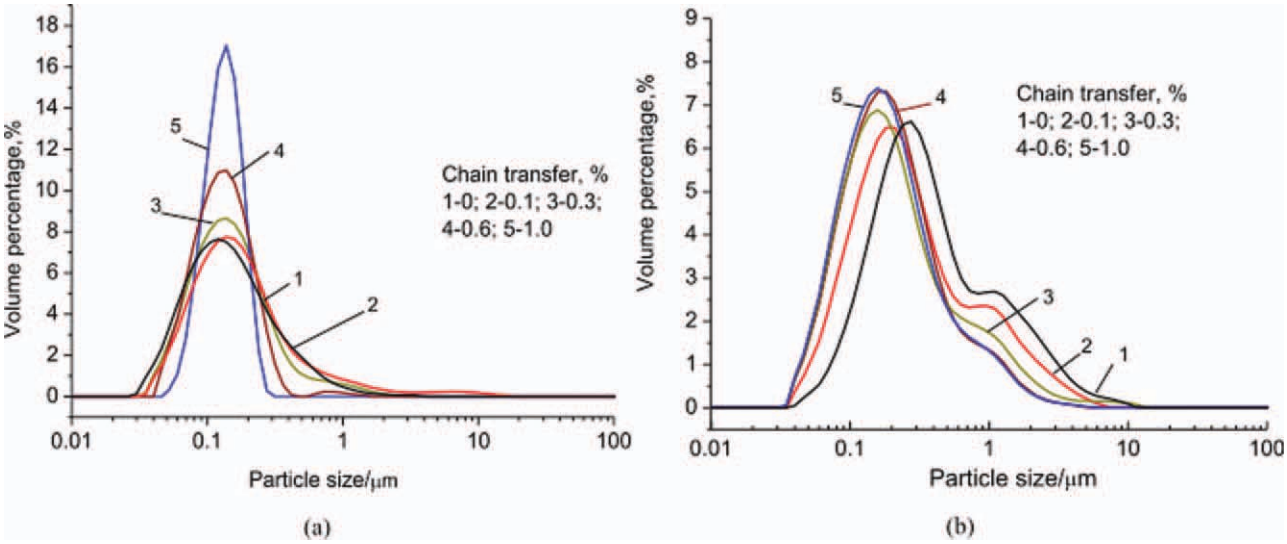

Figure 5 Effect of the concentration of DDM on the particle size distribution of (a) seed particles and (b) core-shell particles. [Color figure can be viewed in the online issue, which is available at wileyonlinelibrary.com.]

operating under conditions where there are no GMA droplets and the aqueous and particle phases have less than their saturation GMA concentrations. There is obviously a range of conditions that fulfill the above requirements of a starved feed system, from a monomer concentration just below that required to saturate the particle and aqueous phases with monomer, down to very low monomer concentrations. In theory, it is possible to reduce the rate of aqueous oligomer growth to a level where all radicals either enter existing particles or terminate. However, there are practical limitations to the degree of starved feed that can be achieved, so that it may not be possible to completely avoid secondary particle formation by this method. One such limitation is mixing. When monomer is added, there will be locations in the reactor where there is an above-average concentration of monomer. This higher concentration of monomer means that in some locations the rate of chain propagation in the aqueous phase is above average, and possibly high enough to result in nucleation of polymer chains. Figure 6 reveals the effect of starved feed of monomer on the morphology of the resulting core-shell emulsion particles.

Comparison of the particle morphologies resulting from different feed rates of GMA monomer in the second stage polymerization (Fig. 7) reveals that smaller feed rate [Fig. 7(c,d)] of GMA was beneficial to the formation of well-defined core-shell structures. By contrast, addition of GMA as a single shot [Fig. 7(a)] or at 40 g h^{-1} [Fig. 7(b)] produced very few core-shell particles. The smaller feed rates reduced the concentration of GMA in the aqueous phase, thereby reducing the propagation rate of aqueous phase radicals so that they were more likely to enter seed latex particles and create core-shell particles, than to undergo secondary nucleation.

Real-time FTIR measurements of isothermal postcrosslinking

A core-shell emulsion containing 11 mol % epoxy group and the amine curing agent was used for these experiments. The ratio of epoxy groups to amino groups was stoichiometric (1 : 1 by mole).

Figure 8 shows a series of FTIR spectra collected at different times after mixing a core-shell emulsion with 11 mol % epoxy groups with Anquamine 419 curing agent at 30°C. Spectra were obtained in the wavenumber range 1320–1690 cm^{-1}. It is apparent that the peak at 1635 cm^{-1}, assigned to the deformation vibration of $-NH_2$, progressively decreased in intensity throughout the crosslinking process and was not detected after about 300 min. Similar behavior was observed at 40°C, except that the 1635 cm^{-1} peak vanished at 120 min, and at 22°C the 1635 cm^{-1} peak did not vanish after 300 min. The band at 1376 cm^{-1} is assigned to the symmetric deformation vibration of methyl groups, and it was assumed that methyl groups were not involved in the crosslinking reaction and hence the area of the 1376 cm^{-1} band did not change over the entire crosslinking period. Consequently, the invariant peak at 1376 cm^{-1} was used in all spectra as an internal normalization standard, and the relative conversion (α) of the epoxy group at a given isothermal curing temperature was evaluated as a function of time from the eq. (2)

$$\alpha = 1 - \{(A_{1635}/A_{1376})_t/(A_{1635}/A_{1376})_{t=0}\} \qquad (2)$$

where A is the absorbance of the reactive species, and t is the crosslinking time.

Figure 9 shows that conversion increased with time at constant curing temperature and was more rapid at higher curing temperatures. After 300 min,

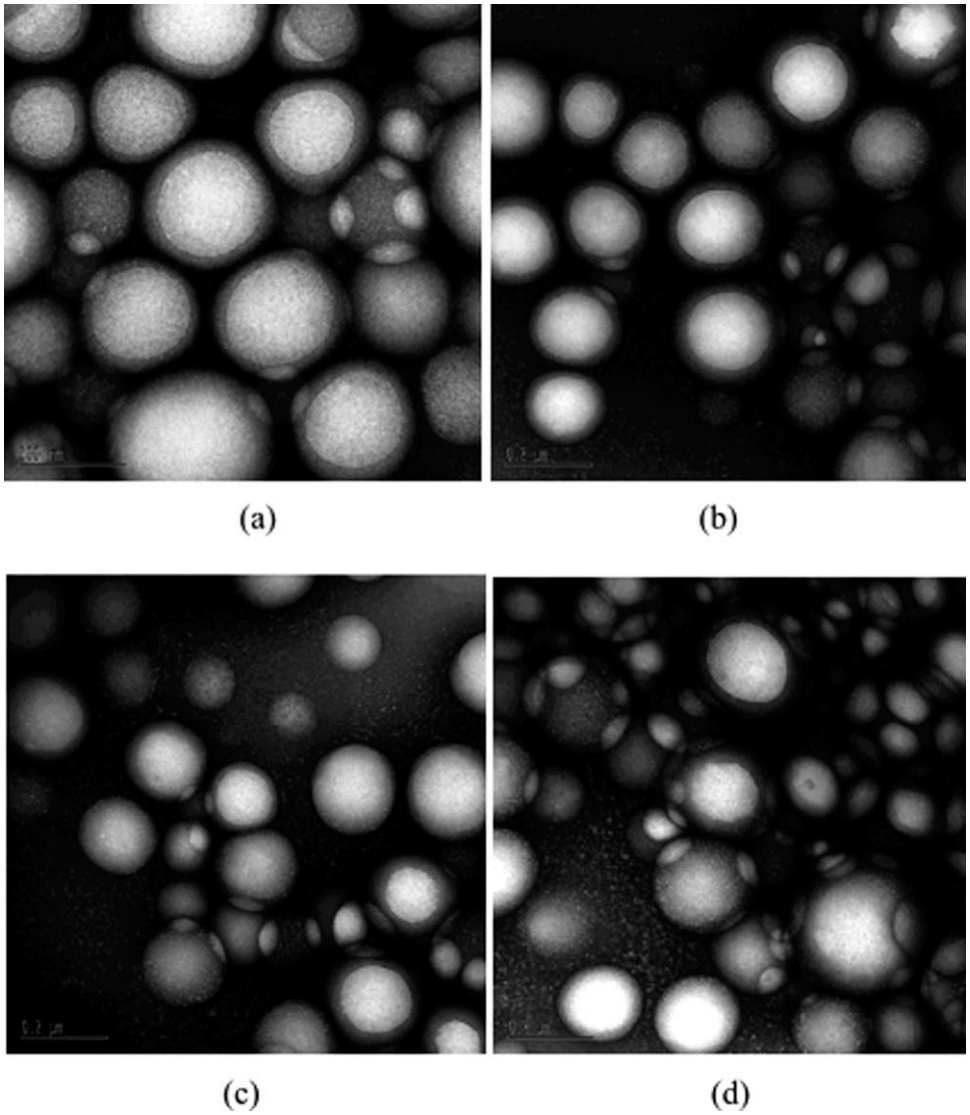

Figure 6 Effect of feed rate of monomer on the morphology of particles (a) add all GMA once; (b) 20 g/h; (c) 40 g/h; (d) 10 g/h.

the relative conversions at 22, 30, and 40°C were about 0.75, 0.92, and 1, respectively, and it is clear that maximum curing was not attained at 22°C. The maximum degree of cure increased, as expected for a thermally activated process, with increased curing temperature.

Figure 10 was derived by taking the first derivative of the relative conversion versus time data. The figure shows that, again as expected, the initial curing rate is higher at higher temperature than at lower temperature, and decreases overall with increasing degree of cure. Two factors contribute to the overall decrease in the curing rate: (a) the number of available crosslinking sites decreases with increasing degree of cure, and (b) as the degree of crosslinking increases the network hinders diffusion of crosslinker to the remaining crosslinking sites. The sharp drop at about 60% cure in the curing rate at 40°C is associated with the reaction-induced transition from rubbery liquid to glass. The reduced reaction rate arises from the resulting diffusional restrictions and change in reaction mechanism from kinetic to diffusion control.[18,19]

CONCLUSIONS

A crosslinkable core-shell latex with poly(VAc-*co*-VeoVa10) cores and polyGMA shell can be synthesized by the technique of starved feed and seeded emulsion polymerization. The number of particles and particle size of the seed latex influence the formation of core-shell morphology in the second stage emulsion polymerization. The emulsifier concentration provides effective control of particle size and number, and core-shell morphology of the final latex

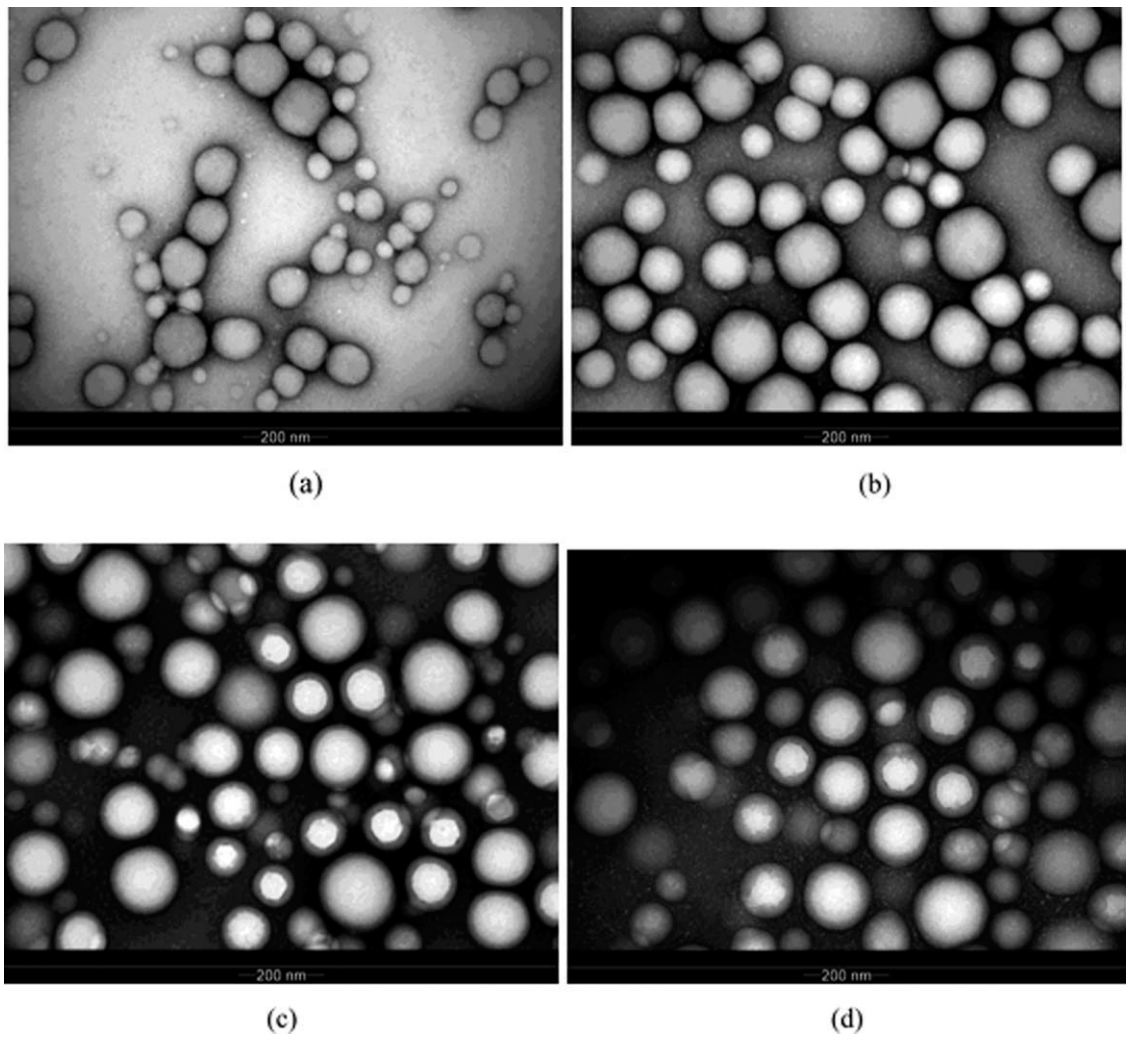

Figure 7 Effect of feed rate of monomer on the morphology of particles (a) add all GMA once; (b) 20 g/h; (c) 40 g/h; (d) 10 g/h.

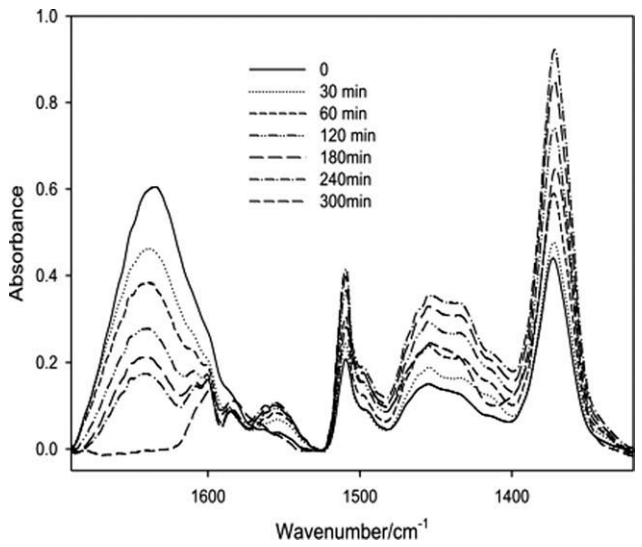

Figure 8 FTIR spectra of mixtures of core-shell emulsion and Anquamine 419 at various times after mixing at 30°C.

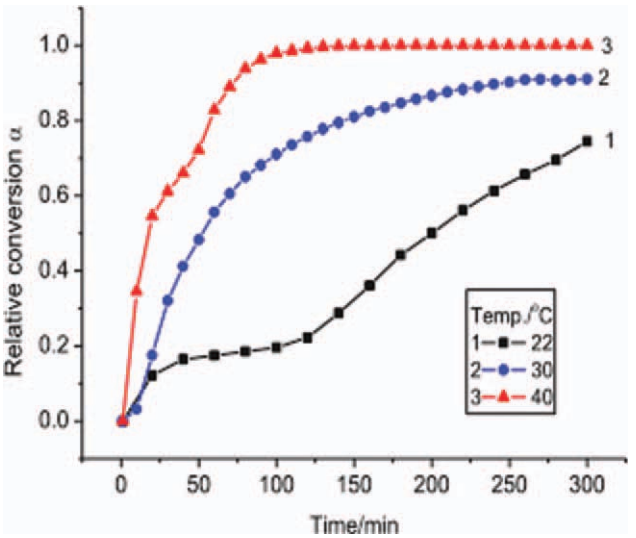

Figure 9 Effect of isothermal temperature on the extent of conversion vs. time for cosslinkable PVAc emulsion and Anquamine 419. [Color figure can be viewed in the online issue, which is available at wileyonlinelibrary.com.]

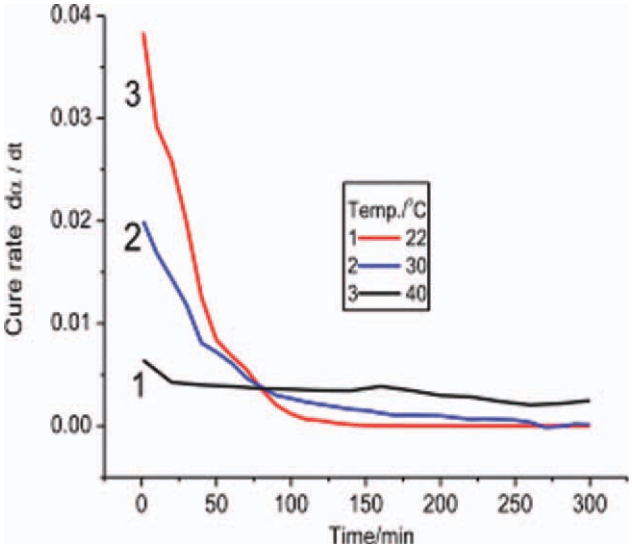

Figure 10 Cure rate as a function of time at different isothermal temperature. [Color figure can be viewed in the online issue, which is available at wileyonlinelibrary.com.]

was favored by higher concentration of emulsifier in the seed latex. Addition of a CTA in the preparation of the seed latex increased the mobility of the seed polymer and subsequently polyGMA chains to the extent that "acorn" (multicore) particles were present to a significant extent in the final core-shell latex. Core-shell particle morphology was facilitated by using a starved feed of GMA in the second stage polymerization, to reduce the rate of propagation and hence the steady state concentration of GMA radicals in the aqueous phase. The quantitative changes in concentration of primary amine groups based on the data of real-time FTIR spectroscopy revealed cure rate was sensitive to the curing temperature and decreased with increasing degree of conversion.

References

1. Grigsby, W. J.; Ferguson, C. J.; France, R. A.; Russell, G. T. Int J Adhes Adhes 2005, 25, 127.
2. Duquesne, S.; Lefebvre, J.; Delobel, R.; Camino, G.; LeBras, M.; Seeley, G. Polym Degrad Stab 2004, 83, 19.
3. Qiao, L.; Easteal, A. J.; Bolt, C. J.; Coveny, P. K.; Franich, R. A. Pigm Resin Technol 2000, 29, 229.
4. Kim, S.; Kim, H. J. Int J Adhes Adhes 2005, 25, 456.
5. Brar, A. S.; Yadav, A. J Polym Sci Part A: Polym Chem 2001, 33, 4051.
6. Ferguson, C. J.; Russell, G. T.; Gilbert, R. G. Polymer 2002, 43, 6371.
7. Ferguson, C. J.; Russell, G. T.; Gilbert, R. G. Polymer 2003, 44, 2607.
8. Ferguson, C. J.; Russell, G. T.; Gilbert, R. G. Polymer 2002, 43, 4557.
9. Perez-Carrillo, L. A.; Puca, M.; Rabelero, M.; Meza, K. E.; Puig, J. E.; Mendizabal, E.; Lopez-Serrano, F.; Lopez, R. G. Polymer, 2007, 48, 1212.
10. Jonsson, J.-E.; Karlsson, O. J.; Hassander, H.; Tornell, B. Eur Polym J 2007, 43, 1322.
11. Olah, A.; Hempenius, M. A.; Vancso, G. J. Eur Polym J 2004, 40, 763.
12. Kirsch, S.; Pfau, A.; Stubbs, J.; Sundberg, D. Colloids Surf A 2001, 183, 725.
13. Kang, K.; Kan, C.; Du, Y.; Liu, D. Eur Polym J 2005, 41, 439.
14. Nomura, M.; Tobita, H.; Suzuki, K. Adv Polym Sci 2005, 175, 128.
15. Suzuki, S.; Kikuchi, K.; Suzuki, A.; Okaya, T.; Nomura, M. Colloid Polym Sci 2007, 285, 523.
16. Barudio, J.; Guillot, G. F. J. Polym Sci Part A: Polym Chem 2000, 36, 157.
17. Zhao, K.; Sun, P.; Liu, D.; Dai, G. Eur Polym J 2004, 40, 89.
18. Dusek, K.; Dusková-Smrcková, M. Progr Polym Sci 2000, 25, 1215.
19. Rocks, J.; Rintoul, L.; Vohwinkel, F.; George, G. Polymer 2004, 45, 6799.